



OPEN

DATA DESCRIPTOR

Datasets of *in vitro* clonogenic assays showing low dose hyper-radiosensitivity and induced radioresistance

Szabolcs Polgár^{1,2}, Paul N. Schofield³ & Balázs G. Madas^{2,4}✉

Low dose hyper-radiosensitivity and induced radioresistance are primarily observed in surviving fractions of cell populations exposed to ionizing radiation, plotted as the function of absorbed dose. Several biophysical models have been developed to quantitatively describe these phenomena. However, there is a lack of raw, openly available experimental data to support the development and validation of quantitative models. The aim of this study was to set up a database of experimental data from the public literature. Using Google Scholar search, 46 publications with 101 datasets on the dose-dependence of surviving fractions, with clear evidence of low dose hyper-radiosensitivity, were identified. Surviving fractions, their uncertainties, and the corresponding absorbed doses were digitized from graphs of the publications. The characteristics of the cell line and the irradiation were also recorded, along with the parameters of the linear-quadratic model and/or the induced repair model if they were provided. The database is available in STORE^{DB}, and can be used for meta-analysis, for comparison with new experiments, and for development and validation of biophysical models.

Background & Summary

Clonogenic assay or colony formation assay is an *in vitro* cell survival assay based on the ability of a single cell to grow into a colony; a colony is defined as having at least 50 cells¹. The surviving fraction (*SF*) of cells as the function of absorbed dose can generally be described by the linear-quadratic (LQ) model² (Eq. 1). In this model, the fraction of surviving cells decreases exponentially as the function of dose, and this exponential function consists of a linear and a quadratic term. As surviving fraction is normalized to the unirradiated control, it equals 100% at 0 Gy by definition:

$$SF = e^{-\alpha D - \beta D^2}, \quad (1)$$

where *D* is the absorbed dose (Gy) and α and β are the linear and quadratic parameters describing the radio-sensitivity of the cells.

For certain cell lines, however, the surviving fraction at low doses significantly differs from the LQ model³. These cell lines exhibit hyper-radiosensitivity (HRS) at very low radiation doses (~0.1 Gy) which is not predicted by extrapolating the cell survival response from higher doses using the LQ model. As the dose increases above ~0.3 Gy, there is an increased radioresistance (IRR) to doses beyond ~1 Gy, where radioresistance is maximal, and cell survival starts to follow the LQ model. As HRS and IRR may have implications for cancer therapy, several biophysical models^{4–8} have been developed, aiming to provide a deeper understanding of the phenomena.

The development and validation of such biophysical models requires raw experimental data, and cell survival data are a key resource in understanding the factors underlying the phenomena of biosensitivity to low dose radiation. Despite improvements in the requirement for authors to make raw data supporting publications

¹Doctoral School of Physics, ELTE Eötvös Loránd University, Budapest, Hungary. ²Environmental Physics Department, Centre for Energy Research, Budapest, Hungary. ³Department of Physiology, Development and Neuroscience, University of Cambridge, Cambridge, United Kingdom. ⁴Department of Physical Chemistry and Materials Science, Budapest University of Technology and Economics, Budapest, Hungary. ✉e-mail: balazs.madas@ek-cer.hu

publicly available, there is still a significant gap between expectation and delivery^{9–11}. Moreover, it is also clear that relying on authors to provide data personally on request is not reliable, and accessibility decreases with time from the data of publication¹². We have addressed this problem by extracting primary data from published graphics in papers, a strategy not so far attempted at scale, and provide that data in a public database together with a demonstration of the power of data integration and reanalysis, supporting key aims of FAIR data which include interoperability and reuse¹³. Reproducibility of published studies is of increasing concern^{14,15} and we demonstrate here how reproducibility can be assessed using data harvested from prior studies.

Friedrich *et al.*¹⁶ established a database, the Particle Irradiation Data Ensemble (PIDE), of cell survival experiments published in the literature. Raw data have been added more recently¹⁷. The focus of their data mining was to support the study of relative biological effectiveness (RBE) for clonogenic cell survival as endpoint, and to provide a benchmark for RBE-predicting models against experimental data. Therefore, only those *in vitro* cell survival experiments are included in PIDE, where data are available on both photon and ion irradiation, excluding important studies of HRS and IRR.

The aims of the present study were to collect datasets featuring experiments with various cell cultures showing HRS and IRR from published articles in a reproducible and technically sound way and make them publicly available according to the FAIR guidelines¹³. Besides raw data on cell survival and absorbed dose, parameters of the most frequently fitted models, the LQ model and the induced repair model (IR model) were also collected. A schematic overview of the study is provided in Fig. 1.

Methods

A literature review was performed using the search tool of Google Scholar (<https://scholar.google.com/>) with the keywords of “low-dose hyper-radiosensitivity”, “low-dose hrs”, and “induced radioresistance”. The references in the articles found were also searched for graphs. The last search was performed on 2nd August 2021. Criteria for a graph to be processed were the following:

- (i) a low-dose HRS region could clearly be identified in the graph,
- (ii) the data points of the surviving fractions and their uncertainties were readable from the graphs, and
- (iii) the axes and the scale of the graphs were clearly visible.

Applying this procedure, 46 articles were found containing 101 datasets^{3,18–62}. The oldest articles were published in 1993, while the most recent ones in 2021, so the datasets were taken from a time span of over 25 years. There were a wide variety of cell lines investigated, and different radiation types and dose rates were applied. Some publications were found with graphs which met criterion (i) but not criterion (ii)^{63–66}.

Since the last search was performed, other publications were found which could have been included in the database^{67–70}. It shows that our search did not find all relevant publications. The database can later be extended with data from these publications.

For each article, the title, the authors, the figure number which the dataset was obtained from, the name of the irradiated cell line, the type of the radiation and its properties (which were characteristic and provided, e.g., dose rate, energy, tube voltage, linear energy transfer) were recorded. If the authors fitted the LQ or the IR model to their data, then those parameters and their standard errors or confidence intervals were also noted, depending on which one was given.

In order to obtain numerical values of surviving fractions, corresponding absorbed doses, and uncertainties of the surviving fractions from the graphs, the applications WebPlotDigitizer4.2 (GNU Affero General Public License v3.0, <https://automeris.io/WebPlotDigitizer/>) and OriginPro2018 (OriginLab Corporation, <https://www.originlab.com/>) were used. First, the x and y axes had to be defined with the scale (linear or logarithmic) and by defining two points known for each to determine the size of one unit. After that, numerical data for surviving fractions and the corresponding absorbed doses could be read from the individual data points. Uncertainties of the surviving fractions were determined by reading the minimum and maximum values of the whiskers of each data points. As there is no unique established way of reporting errors in cell survival values¹⁶, uncertainty of surviving fraction may mean standard deviation or standard error of the mean, and in some cases it is not even mentioned which one was used. For the LQ and IR model fits, the parameters are presented either with standard errors or confidence intervals depending on the preference of the authors. While these two could be calculated from each other, the required information for this is frequently not presented in the article.

To validate the numerical value of the LQ and IR model fits in the articles, a reanalysis was performed on the actual datasets. The LQ model fit was given by the original articles in a total of 24 cases and the IR model fit was given in a total of 59 cases, the results of the reanalysis were compared to the published data. Our fit was considered to be different from the original one if the difference between values of any IR parameters (α_r , α_s , β , and D_c) was larger than the sum of their uncertainties. The Levenberg–Marquardt method^{71,72} and the Orthogonal Distance Regression⁷³ were used for fitting in the application of OriginPro2018 (OriginLab Corporation, <https://www.originlab.com/>).

In the LQ model, there are two parameters (α and β). As the LQ model does not take into account low dose HRS, Eq. (1) was fitted first only to data points above 1 Gy or to the three data points at the highest doses even if any of them were lower than 1 Gy. If this initial fit did not result in the parameters given in the articles, the Eq. (1) was fitted to the entire dataset including the HRS region.

In the IR model^{37,74}, the relationship between surviving fraction and absorbed dose can be described by Eq. (2):

$$SF = e^{-\alpha_r \left(1 + \left(\frac{\alpha_s}{\alpha_r} - 1 \right) e^{-\frac{D}{D_c}} \right) D - \beta D^2} \quad (2)$$

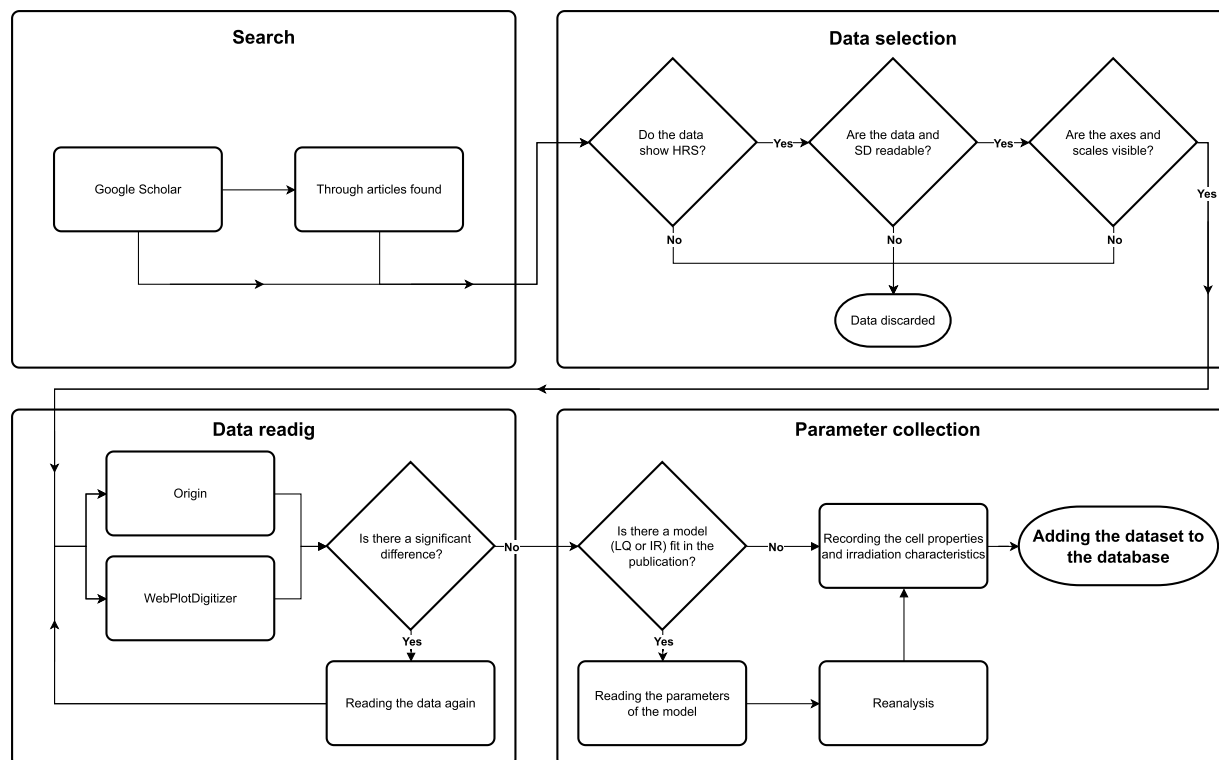


Fig. 1 The flow chart describing the steps we used to acquire the datasets for the database.

Here, β is the same as in the LQ model, while α of the LQ model is replaced by α_r for high doses, and α_s for low doses. D_c is the critical dose or the “transition point” between low-dose hyper-radiosensitivity and induced radioresistance (i.e., when α_s to α_r is 63% complete). As there are four parameters, convergence of the fitting is sensitive to the initial values of the parameters. In order to test whether a fitting method can be found which reproduces the parameters given in the articles, the following protocol was applied, which is also shown in Fig. 2. If one step failed to reproduce the original parameters, the next one was applied.

- 1) The initial values of α_r and β parameters were determined by fitting the LQ model to the surviving fractions measured at absorbed doses higher than 1 Gy, or to the three data points at the highest doses even if any of them were lower than 1 Gy. The initial values of α_s and D_c were set to 1 Gy^{-1} and 1 Gy, respectively. Equation (2) was fit with these four initial values to surviving fractions considering their uncertainty.
- 2) The initial values of the four parameters were set equal to the parameters in the original publications. Equation (2) was fitted to surviving fractions considering their uncertainty.
- 3) The initial values were the same as in 1). Equation (2) was fitted to surviving fractions without considering their uncertainty.
- 4) The initial values were the same as in 2). Equation (2) was fitted to surviving fractions without considering their uncertainty.
- 5) The initial values were the same as in 1). The logarithm of Eq. (2) was fitted to the logarithm of the surviving fractions without considering their uncertainty.
- 6) The initial values were the same as in 2). The logarithm of Eq. (2) was fitted to the logarithm of the surviving fractions without considering their uncertainty.
- 7) Instead of the Levenberg – Marquardt algorithm, the Orthogonal Distance Regression method was applied. The six previous steps were tested until one reproduced the original parameters.
- 8) The seven previous steps were tested until one reproduced the original parameters with one parameter fixed, and the others fitted. The motivation behind this step is that it is easier to find an optimum with fewer parameters fitted simultaneously.
 - a) If the β parameter was negative from the LQ fit, then it was fixed to 0 and the others were fitted.
 - b) Otherwise, the α_r parameter was fixed to the value α of the LQ model fit, and the other parameters were fitted.

Data Records

The first and second versions of the database have been uploaded to the STORE^{DB} database (https://www.storedb.org/store_v3/index.jsp), which is a repository for data and links to resources of the international radiobiology community, and maintained by the Federal Office of Radiation Protection, Germany⁷⁵. It ensures long-term persistence and preservation of datasets, provides deposited datasets with Digital Object Identifiers,

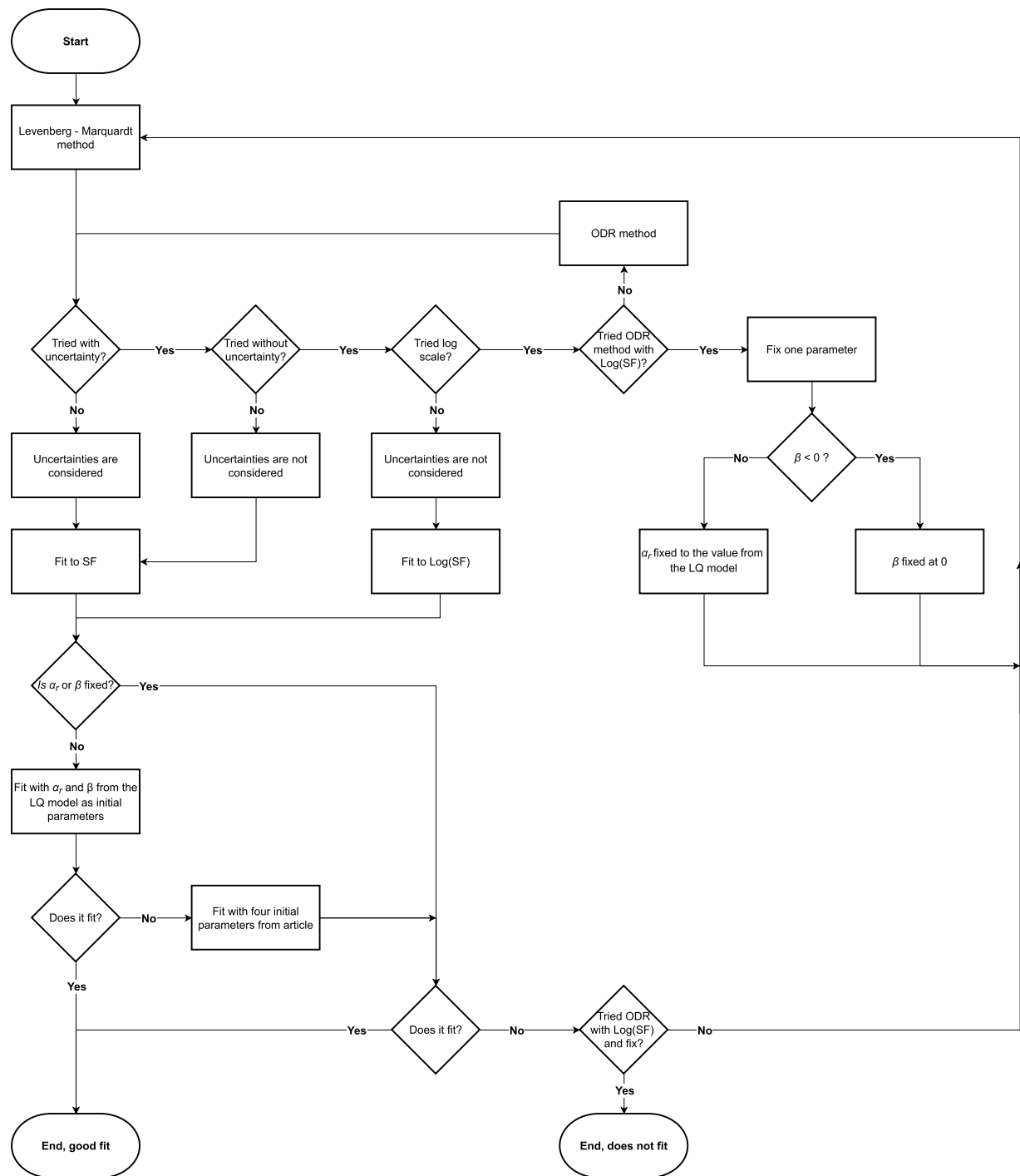


Fig. 2 The flow chart describing the fitting method we used to reproduce the IR model parameters of the original articles.

standardised metadata^{76,77}, allows access to data without unnecessary restrictions, and provides a licence on each dataset landing page.

The current (second) version (STOREDB:DATASET1252) of the database⁷⁸ contains 101 datasets from 46 articles^{3,18–62} in Microsoft Excel 2016 format (Microsoft Corporation, <https://www.microsoft.com/en-gb/microsoft-365/excel>). It is publicly available under Creative Commons Attribution license. One dataset contains the surviving fraction of the cell culture (column C) at a given dose in Gy (column B) and the minimum (column D) and maximum value (column E) of the whiskers of the uncertainty of the surviving fraction. The parameters of the fitted function are also recorded if they were given in the original article, either parameters of the LQ model or the IR model or both. The fit type is given in column G. From column H to column X, the different parameters (columns H, L, P, Q, U) are given with their standard errors (columns I, M, R, V) or confidence limits (columns J, K, N, O, S, T, W, X). In column H, α refers to the LQ fit, while α_r to the IR fit. If there are

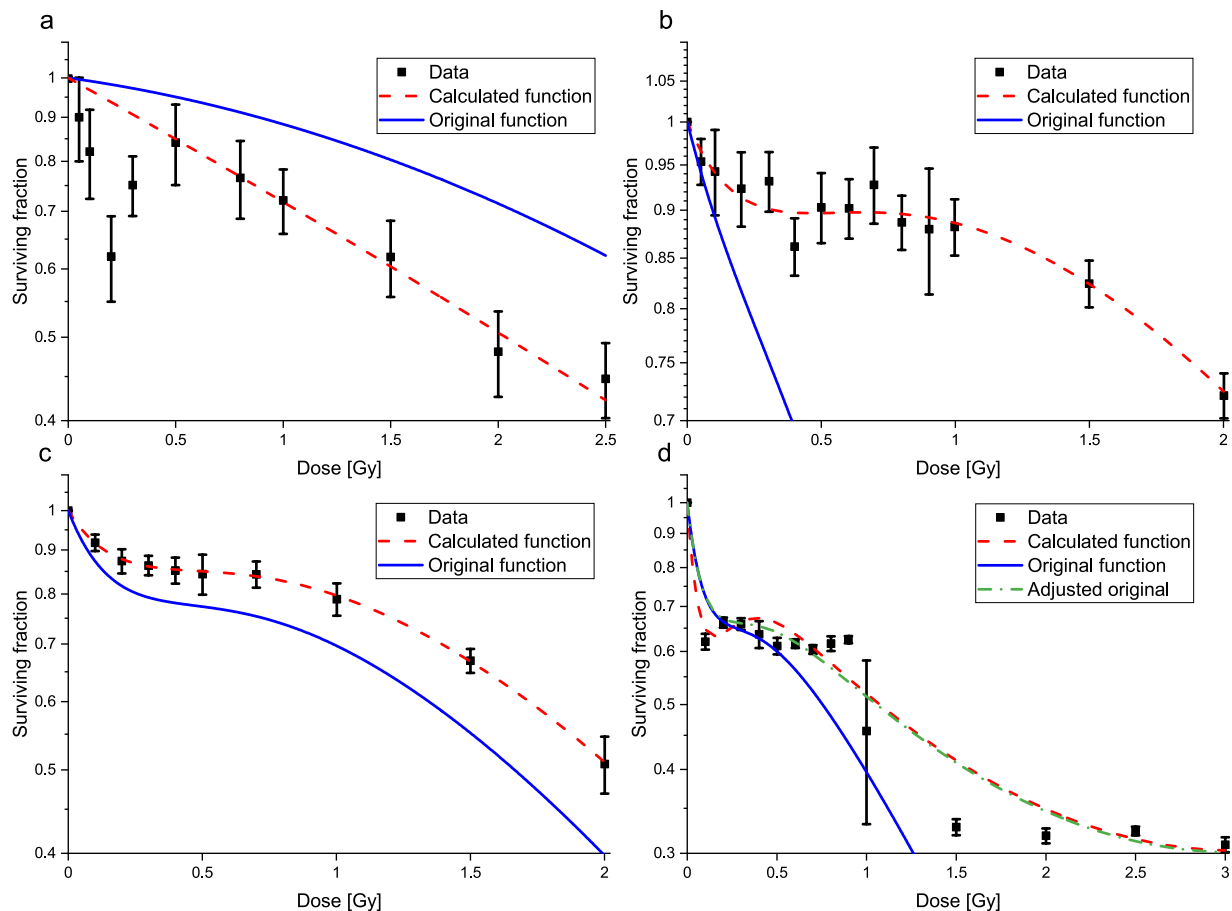


Fig. 3 The graphs show the LQ (panel a) and IR (panels b, c, and d) model fits from the original articles, and from the reanalysis we performed. The original models are presented as blue solid lines, while our fit results as red stripped lines. The experimental data are shown as black squares with their uncertainties. The top left panel (a)⁵⁹ shows the case where the original LQ fit differed from the one of the reanalysis. The top right (b)³³ and bottom left panel (c)⁶¹ show two IR model cases where we could not reproduce the results of the original fit. In case of the bottom right panel (d)³⁴, the original fit results could not be reproduced either. However, if the original parameters with a negated β value are used, then the curve (green dotted line) fits well to the experimental data.

		α (Mean \pm SD)		β (Mean \pm SD)	
a	Original	0.08*	—	0.044	—
	Calculated	0.32*	± 0.11	0.008	± 0.05
		α_r (Mean \pm SD)	β (Mean \pm SD)	α_s (Mean \pm SD)	D_c (Mean \pm SD)
b	Original	$0.49^* \pm 0.11$	$0.52^* \pm 0.26$	1.27 ± 1.18	0.31 ± 0.19
	Calculated	$0.005^* \pm 0.072$	$0.077^* \pm 0.036$	0.787 ± 0.206	0.333 ± 0.107
c	Original	$0.18^* \pm 0.01$	0.14 ± 0.04	$1.86^* \pm 0.05$	0.27 ± 0.08
	Calculated	$0.043^* \pm 0.023$	0.146 ± 0.013	$1.181^* \pm 0.052$	0.296 ± 0.02
d	Original	0.79 ± 0.05	$0.13^* \pm 0.02$	5.45 ± 1.35	0.15 ± 0.03
	Calculated	0.783 ± 0.068	$-0.128^* \pm 0.028$	9.233 ± 4.191	0.115 ± 0.033

Table 1. Differences between the LQ (row a⁵⁹) and IR (rows b³³, c⁶¹, and d³⁴) model parameters in the original articles and those obtained by fitting the data read. Those parameters are marked with an asterisk (*) where there is a significant difference between the original and our calculated values. In case of the original values of row a, uncertainties were not provided in the article.

parameters or values which were not given in the articles (or no fits were made), then it is indicated with an ‘X’ symbol. If the parameters has no meaning for the given fit (for example the LQ model has only two parameters, α and β , so the others are not applicable), a ‘-’ symbol is used. Lastly, the cell type (the name of cell line, the species, the organ, the cancer type if applicable) in column Z and the characteristics of the irradiation in column AA are recorded (radiation type, dose rate, energy, tube voltage, linear energy transfer, etc.).

Technical Validation

The technical quality of the original data, (i.e., the points in the graphs) are corroborated by the peer-review and publication processes of the journals. The 46 articles processed were published in 17 journals. In December 2021, 15 of them covering 44 articles were indexed by both Web of Science (Science Citation Index Expanded, <https://mjl.clarivate.com>) and Scopus (https://service.elsevier.com/app/answers/detail/a_id/14834/supporthub/scopus). One article²¹ was published in a journal which was not indexed by any of them, while another article²² was published in a journal which was not indexed by Scopus, but was indexed by Web of Science (Emerging Sources Citation Index). Before using the data, however, users of the database should review the original publications, whether the materials and methods used to generate the original data meets the requirements of the usage they plan.

Regarding the most important aspects however, the protocols used for data generation were consistent. The definition of surviving cells was the same in all except one publication⁴³. Those cells were considered as survivors, which was able to generate a colony with more than 50 cells after irradiation. While three articles^{47,54,60} do not include this definition of colony formation, the authors of these articles used the same definition in their other publications^{49,59,62}. If plating efficiency was mentioned in the article, then it was also stated that surviving fractions after irradiation was calculated considering the plating efficiency of the control i.e., non-irradiated cells. These are in agreement with the protocol of the clonogenic assay described by Franken *et al.*¹.

On the other hand, differences in the protocols were also found during the review of the Materials and Methods sections. In some cases, the cell cycles of the cells were synchronized, e.g. in³⁴, while in other cases they were exposed to hormonal treatment²⁹. The time between plating and irradiation also varied cf²³. and⁴⁴. In addition, cell counting was performed either by hand⁴⁹ or by a computer program³⁴.

The technical quality of the collected data was ensured by using two different software for data collection. If there was a larger difference than 0.01 between the numerical values of surviving fractions read by WebPlotDigitizer4.2 and OriginPro2018, the data point was digitized again from the original graphs by both applications. The same quality control procedure was applied to the whiskers. In the case of absorbed doses, it was also considered that the dose values are integer multiples of 0.05 Gy.

While it was a condition for the data to be included in the database that uncertainties of surviving fractions were reported, it is important to note that there is no unique established way of reporting errors in cell survival values¹⁶. In addition, they still represent only a lower limit concerning the uncertainty of the data and a full uncertainty analysis would be demanding as both stochastic and systematic errors would have to be respected¹⁶.

In order to ensure the technical quality of the LQ and IR model parameters, a reanalysis was performed by fitting to the digitized data. The LQ model fit converged in all the 101 datasets. The LQ model parameters were provided in the original articles only in 24 cases. From these 24, there was only one dataset⁵⁹ where the parameters obtained by our fit and the parameters of the original article were significantly different.

Our IR model fit did not converge in case of 15 datasets from the total of 101. IR model parameters were not provided in the original articles in case of these 15 datasets. From the remaining 86 datasets where our IR model fit converged, there were 59, where the IR parameters were provided in the original articles. In case of 56 datasets, one of the methods reproduced the original parameters. In case of the remaining three datasets, the original IR parameters could not be reproduced by the fitting procedure we applied. The differences in these three cases can be seen in Fig. 3 as well as in Table 1 (panels and rows b³³, c⁶¹, and d³⁴).

Usage Notes

The database can be used for meta-analysis, model validation, or for comparison with the results of new experiments. Users can download the Microsoft Excel 2016 file. It contains a single sheet with all the 101 datasets. Users can search for radiation type (e.g., ⁴He²⁺ or X-rays) or for cell line (e.g., CHO or V79) using the search tool of the application and select relevant datasets for their studies. Datasets can be copied and pasted into other applications where they can be analysed or compared with model predictions or new experimental data. While the database is significantly smaller than the Particle Irradiation Data Ensemble¹⁷, it may also be useful for the systematic analysis of the datasets included.

Code availability

No custom code was used to generate or process the data. WebPlotDigitizer4.2 (GNU Affero General Public License v3.0, <https://automeris.io/WebPlotDigitizer/>) and OriginPro2018 (OriginLab Corporation, <https://www.originlab.com/>) were used to obtain numerical values of the data points and their uncertainties plotted in the graphs. The file containing the database was prepared in Microsoft Excel 2016 (Microsoft Corporation, <https://www.microsoft.com/en-gb/microsoft-365/excel>).

Received: 21 May 2022; Accepted: 19 August 2022;

Published online: 08 September 2022

References

1. Franken, N. A. P., Rodermond, H. M., Stap, J., Haveman, J. & van Bree, C. Clonogenic assay of cells *in vitro*. *Nat. Protoc.* **1**, 2315–2319 (2006).
2. Hall, E. J. & Giaccia, A. J. *Radiobiology for the radiologist*. (Wolters Kluwer Health/Lippincott Williams & Wilkins, 2012).
3. Joiner, M. C., Marples, B., Lambin, P., Short, S. C. & Turesson, I. Low-dose hypersensitivity: current status and possible mechanisms. *Int. J. Radiat. Oncol.* **49**, 379–389 (2001).
4. Madas, B. G. & Drozdik, E. J. Computational modelling of low dose hyper-radiosensitivity applying the principle of minimizing mutation rate. *Radiat. Prot. Dosimetry* **183**, 147–150 (2019).
5. Matsuya, Y., Sasaki, K., Yoshii, Y., Okuyama, G. & Date, H. Integrated modelling of cell responses after irradiation for DNA-targeted effects and non-targeted effects. *Sci. Rep.* **8**, 4849 (2018).

6. Olobatuyi, O., de Vries, G. & Hillen, T. A reaction–diffusion model for radiation-induced bystander effects. *J. Math. Biol.* **75**, 341–372 (2017).
7. Olobatuyi, O., de Vries, G. & Hillen, T. Effects of G2-checkpoint dynamics on low-dose hyper-radiosensitivity. *J. Math. Biol.* **77**, 1969–1997 (2018).
8. Powathil, G. G., Munro, A. J., Chaplain, M. A. J. & Swat, M. Bystander effects and their implications for clinical radiation therapy: Insights from multiscale in silico experiments. *J. Theor. Biol.* **401**, 1–14 (2016).
9. Tenopir, C. *et al.* Data sharing, management, use, and reuse: Practices and perceptions of scientists worldwide. *PLOS ONE* **15**, e0229003 (2020).
10. Digital Science *et al.* The State of Open Data 2020. *Digital Science* <https://doi.org/10.6084/M9.FIGSHARE.13227875.V2> (2020).
11. Madas, B. G. & Schofield, P. N. Survey on data management in radiation protection research. *Radiat. Prot. Dosimetry* **183**, 233–236 (2019).
12. Vines, T. H. *et al.* The availability of research data declines rapidly with article age. *Curr. Biol.* **24**, 94–97 (2014).
13. Wilkinson, M. D. *et al.* The FAIR Guiding Principles for scientific data management and stewardship. *Sci. Data* **3**, 160018 (2016).
14. Collins, F. S. & Tabak, L. A. Policy: NIH plans to enhance reproducibility. *Nature* **505**, 612–613 (2014).
15. Ioannidis, J. P. A. How to make more published research true. *PLOS Med.* **11**, e1001747 (2014).
16. Friedrich, T., Scholz, U., Elsässer, T., Durante, M. & Scholz, M. Systematic analysis of RBE and related quantities using a database of cell survival experiments with ion beam irradiation. *J. Radiat. Res.* **54**, 494–514 (2012).
17. Friedrich, T., Pfuhl, T. & Scholz, M. Update of the particle irradiation data ensemble (PIDE) for cell survival. *J. Radiat. Res.* **62**, 645–655 (2021).
18. Beauchesne, P. D. *et al.* Human malignant glioma cell lines are sensitive to low radiation doses. *Int. J. Cancer* **105**, 33–40 (2003).
19. Böhrens, G., J. Weber, K. & Scholz, M. Low dose hypersensitivity and induced resistance of V79 cells after charged particle irradiation using 100 MeV/u carbon ions. *Radiat. Prot. Dosimetry* **99**, 255–256 (2002).
20. Chalmers, A., Johnston, P., Woodcock, M., Joiner, M. & Marples, B. PARP-1, PARP-2, and the cellular response to low doses of ionizing radiation. *Int. J. Radiat. Oncol.* **58**, 410–419 (2004).
21. Dai, X., Tao, D., Wu, H. & Cheng, J. Low dose hyper-radiosensitivity in human lung cancer cell line A549 and its possible mechanisms. *J. Huazhong Univ. Sci. Technolog. Med. Sci.* **29**, 101–106 (2009).
22. Das, S. Radiobiological response of cervical cancer cell line in low dose region: evidence of low dose hypersensitivity (HRS) and induced radioresistance (IRR). *J. Clin. Diagn. Res.* <https://doi.org/10.7860/JCDR/2015/14120.6074> (2015).
23. Dionet, C. *et al.* Effects of low-dose neutrons applied at reduced dose rate on human melanoma cells. *Radiat. Res.* **154**, 406–411 (2000).
24. Edin, N. J. *et al.* Mechanisms of the elimination of low dose hyper-radiosensitivity in T-47D cells by low dose-rate priming. *Int. J. Radiat. Biol.* **85**, 1157–1165 (2009).
25. Edin, N. J., Olsen, D. R., Sandvik, J. A., Malinen, E. & Pettersen, E. O. Low dose hyper-radiosensitivity is eliminated during exposure to cycling hypoxia but returns after reoxygenation. *Int. J. Radiat. Biol.* **88**, 311–319 (2012).
26. Fernandez-Palomo, C., Seymour, C. & Mothersill, C. Inter-relationship between low-dose hyper-radiosensitivity and radiation-induced bystander effects in the human T98G glioma and the epithelial HaCaT cell line. *Radiat. Res.* **185**, 124–133 (2016).
27. Guirado, D. *et al.* Low-dose radiation hyper-radiosensitivity in multicellular tumour spheroids. *Br. J. Radiol.* **85**, 1398–1406 (2012).
28. Hanu, C. *et al.* Low-dose non-targeted radiation effects in human esophageal adenocarcinoma cell lines. *Int. J. Radiat. Biol.* **93**, 165–173 (2017).
29. Hermann, R. M. *et al.* *In vitro* studies on the modification of low-dose hyper-radiosensitivity in prostate cancer cells by incubation with genistein and estradiol. *Radiat. Oncol.* **3**, 19 (2008).
30. Heuskin, A.-C., Wéra, A.-C., Riquier, H., Michiels, C. & Lucas, S. Low-dose hypersensitivity and bystander effect are not mutually exclusive in A549 lung carcinoma cells after irradiation with charged particles. *Radiat. Res.* **180**, 491–498 (2013).
31. Jin, X. *et al.* The hyper-radiosensitivity effect of human hepatoma SMMC-7721 cells exposed to low dose γ -rays and 12C ions. *Nucl. Instrum. Methods Phys. Res. Sect. B Beam Interact. Mater. At.* **245**, 310–313 (2006).
32. Joiner, M. C. *et al.* Hypersensitivity to very-low single radiation doses: Its relationship to the adaptive response and induced radioresistance. *Mutat. Res. Mol. Mech. Mutagen.* **358**, 171–183 (1996).
33. Krueger, S. A., Joiner, M. C., Weinfeld, M., Piasentin, E. & Marples, B. Role of apoptosis in low-dose hyper-radiosensitivity. *Radiat. Res.* **167**, 260–267 (2007).
34. Krueger, S. A., Wilson, G. D., Piasentin, E., Joiner, M. C. & Marples, B. The effects of G2-phase enrichment and checkpoint abrogation on low-dose hyper-radiosensitivity. *Int. J. Radiat. Oncol.* **77**, 1509–1517 (2010).
35. Lambin, P., Marples, B., Fertil, B., Malaise, E. P. & Joiner, M. C. Hypersensitivity of a human tumour cell line to very low radiation doses. *Int. J. Radiat. Biol.* **63**, 639–650 (1993).
36. Maeda, M., Usami, N. & Kobayashi, K. Low-dose hypersensitivity in nucleus-irradiated V79 cells studied with synchrotron X-ray microbeam. *J. Radiat. Res.* **49**, 171–180 (2008).
37. Marples, B. & Joiner, M. C. The response of Chinese hamster V79 cells to low radiation doses: evidence of enhanced sensitivity of the whole cell population. *Radiat. Res.* **133**, 41 (1993).
38. Marples, B. & Joiner, M. C. The elimination of low-dose hypersensitivity in Chinese hamster V79-379A cells by pretreatment with X rays or hydrogen peroxide. *Radiat. Res.* **141**, 160 (1995).
39. Marples, B., Cann, N. E., Mitchell, C. R., Johnston, P. J. & Joiner, M. C. Evidence for the involvement of DNA-dependent protein kinase in the phenomena of low dose hyper-radiosensitivity and increased radioresistance. *Int. J. Radiat. Biol.* **78**, 1139–1147 (2002).
40. Marples, B., Wouters, B. G. & Joiner, M. C. An association between the radiation-induced arrest of G₂-phase cells and low-dose hyper-radiosensitivity: a plausible underlying mechanism? *Radiat. Res.* **160**, 38–45 (2003).
41. Marples, B., Wouters, B. G., Collis, S. J., Chalmers, A. J. & Joiner, M. C. Low-dose hyper-radiosensitivity: a consequence of ineffective cell cycle arrest of radiation-damaged G₂-phase cells. *Radiat. Res.* **161**, 247–255 (2004).
42. Martin, L. *et al.* Recognition of O6MEG lesions by MGMT and mismatch repair proficiency may be a prerequisite for low-dose radiation hypersensitivity. *Radiat. Res.* **172**, 405–413 (2009).
43. Nagle, P. W. *et al.* Lack of DNA damage response at low radiation doses in adult stem cells contributes to organ dysfunction. *Clin. Cancer Res.* **12**.
44. Nuta, O. & Darrroudi, F. The impact of the bystander effect on the low-dose hypersensitivity phenomenon. *Radiat. Environ. Biophys.* **47**, 265–274 (2008).
45. Schettino, G. *et al.* Low-dose studies of bystander cell killing with targeted soft X rays. *Radiat. Res.* **160**, 505–511 (2003).
46. Schoenherr, D. *et al.* Determining if low dose hyper-radiosensitivity (HRS) can be exploited to provide a therapeutic advantage: A cell line study in four glioblastoma multiforme (GBM) cell lines. *Int. J. Radiat. Biol.* **89**, 1009–1016 (2013).
47. Short, S., Mayes, C., Woodcock, M., Johns, H. & Joiner, M. C. Low dose hypersensitivity in the T98G human glioblastoma cell line. *Int. J. Radiat. Biol.* **75**, 847–855 (1999).
48. Short, S. C., Mitchell, S. A., Boulton, P., Woodcock, M. & Joiner, M. C. The response of human glioma cell lines to low-dose radiation exposure. *Int. J. Radiat. Biol.* **75**, 1341–1348 (1999).
49. Short, S. C., Woodcock, M., Marples, B. & Joiner, M. C. Effects of cell cycle phase on low-dose hyper-radiosensitivity. *Int. J. Radiat. Biol.* **79**, 99–105 (2003).

50. Skov, K., Marples, B., Matthews, J. B., Joiner, M. C. & Zhou, H. A preliminary investigation into the extent of increased radioresistance or hyper-radiosensitivity in cells of hamster cell lines known to be deficient in DNA repair. *Radiat. Res.* **138**, S126 (1994).
51. Stonina, D. *et al.* Low-dose hyper-radiosensitivity is not a common effect in normal asynchronous and G2-phase fibroblasts of cancer patients. *Int. J. Radiat. Oncol.* **88**, 369–376 (2014).
52. Stonina, D., Gasińska, A., Biesaga, B., Janecka, A. & Kabat, D. An association between low-dose hyper-radiosensitivity and the early G2-phase checkpoint in normal fibroblasts of cancer patients. *DNA Repair* **39**, 41–45 (2016).
53. Stonina, D., Kabat, D., Biesaga, B., Janecka-Widła, A. & Szatkowski, W. Chemopotentiating effects of low-dose fractionated radiation on cisplatin and paclitaxel in cervix cancer cell lines and normal fibroblasts from patients with cervix cancer. *DNA Repair* **103**, 103113 (2021).
54. Toulou, E., Baggio, L., Cherubini, R. & Kalfas, A. C. Radiosensitivity of V79 cells after alpha particle radiation at low doses. *Radiat. Prot. Dosimetry* **99**, 237–240 (2002).
55. Wang, Q. *et al.* The role and mechanism of ATM-mediated autophagy in the transition from hyper-radiosensitivity to induced radioresistance in lung cancer under low-dose radiation. *Front. Cell Dev. Biol.* **9**, 650819 (2021).
56. Wéra, A.-C. *et al.* Comparison of the clonogenic survival of A549 non-small cell lung adenocarcinoma cells after irradiation with low-dose-rate beta particles and high-dose-rate X-rays. *Int. J. Radiat. Biol.* **88**, 253–257 (2012).
57. Wouters, B. G., Sy, A. M. & Skarsgard, L. D. Low-dose hypersensitivity and increased radioresistance in a panel of human tumor cell lines with different radiosensitivity. *Radiat. Res.* **146**, 399 (1996).
58. Wykes, S. M., Piasentin, E., Joiner, M. C., Wilson, G. D. & Marples, B. Low-dose hyper-radiosensitivity is not caused by a failure to recognize DNA double-strand breaks. *Radiat. Res.* **165**, 516–524 (2006).
59. Xue, J. *et al.* Low-dose hyper-radiosensitivity in human hepatocellular HepG2 cells is associated with Cdc25C-mediated G2/M cell cycle checkpoint control. *Int. J. Radiat. Biol.* **92**, 543–547 (2016).
60. Xue, L. *et al.* ATM-dependent hyper-radiosensitivity in mammalian cells irradiated by heavy ions. *Int. J. Radiat. Oncol.* **75**, 235–243 (2009).
61. Zhao, Y. *et al.* Cell division cycle 25 homolog c effects on low-dose hyper-radiosensitivity and induced radioresistance at elevated dosage in A549 cells. *J. Radiat. Res.* **53**, 686–694 (2012).
62. Toulou, E., Baggio, L., Cherubini, R. & Kalfas, C. A. Low-dose hypersensitivity of V79 cells under exposure to γ -rays and 4 He ions of different energies: survival and chromosome aberrations. *Int. J. Radiat. Biol.* **77**, 1133–1139 (2001).
63. Enns, L., Rasouli-Nia, A., Hendzel, M., Marples, B. & Weinfeld, M. Association of ATM activation and DNA repair with induced radioresistance after low-dose irradiation. *Radiat. Prot. Dosimetry* **166**, 131–136 (2015).
64. Fernet, M., Mégnin-Chanet, F., Hall, J. & Favaudon, V. Control of the G2/M checkpoints after exposure to low doses of ionising radiation: Implications for hyper-radiosensitivity. *DNA Repair* **9**, 48–57 (2010).
65. Ryan, L. A., Seymour, C. B., Joiner, M. C. & Mothersill, C. E. Radiation-induced adaptive response is not seen in cell lines showing a bystander effect but is seen in lines showing HRS/IRR response. *Int. J. Radiat. Biol.* **85**, 87–95 (2009).
66. Ye, F. *et al.* The influence of non-DNA-targeted effects on carbon ion-induced low-dose hyper-radiosensitivity in MRC-5 cells. *J. Radiat. Res.* **57**, 103–109 (2016).
67. Cherubini, R., De Nadal, V. & Gerardi, S. Hyper-radiosensitivity and induced radioresistance and bystander effects in rodent and human cells as a function of radiation quality. *Radiat. Prot. Dosimetry* **166**, 137–141 (2015).
68. Thomas, C. *et al.* Low-dose hyper-radiosensitivity of progressive and regressive cells isolated from a rat colon tumour: impact of DNA repair. *Int. J. Radiat. Biol.* **84**, 533–548 (2008).
69. Thomas, C. *et al.* Impact of dose-rate on the low-dose hyper-radiosensitivity and induced radioresistance (HRS/IRR) response. *Int. J. Radiat. Biol.* **89**, 813–822 (2013).
70. Xue, L., Furusawa, Y. & Yu, D. ATR signaling cooperates with ATM in the mechanism of low dose hypersensitivity induced by carbon ion beam. *DNA Repair* **34**, 1–8 (2015).
71. Levenberg, K. A method for the solution of certain non-linear problems in least squares. *Q. Appl. Math.* **2**, 164–168 (1944).
72. Marquardt, D. W. An algorithm for least-squares estimation of nonlinear parameters. *J. Soc. Ind. Appl. Math.* **11**, 431–441 (1963).
73. Boggs, P. T. & Byrd, R. H. A stable and efficient algorithm for nonlinear orthogonal distance regression. *SIAM J. Sci. Stat. Comput.* **8**, 1052–1078 (1987).
74. Joiner, M. C. & Johns, H. Renal damage in the mouse: the response to very small doses per fraction. *Radiat. Res.* **114**, 385–398 (1988).
75. Schofield, P. N., Kulka, U., Tapio, S. & Grosche, B. Big data in radiation biology and epidemiology; an overview of the historical and contemporary landscape of data and biomaterial archives. *Int. J. Radiat. Biol.* **95**, 861–878 (2019).
76. The Radiobiology Informatics Consortium. The Radiation Biology Ontology. *GitHub repository* <https://github.com/Radiobiology-Informatics-Consortium> (2022).
77. The Radiobiology Informatics Consortium. Radiation Biology Ontology. *The OBO Foundry* <https://obofoundry.org/ontology/rbo.html> (2022).
78. Polgár, S., Schofield, P. N. & Madas, B. G. Data collection and analysis on low dose hyper-radiosensitivity and induced radioresistance, *StoreDB*, <https://doi.org/10.20348/STOREDB/1163> (2021).

Acknowledgements

This study is part of the RadoNorm project which has received funding from the Euratom research and training programme 2019–2020 under grant agreement No 900009. The study was also supported by the Hungarian Research Data Alliance and the Library and Information Centre of the Hungarian Academy of Sciences (Centre for Energy Research, 21–61), the János Bolyai Research Scholarship of the Hungarian Academy of Sciences (BGM, bo-37-2021), and the ÚNKP-21-5 New National Excellence Program of the Ministry for Innovation and Technology from the source of the National Research, Development and Innovation Fund (BGM, ÚNKP-21-5-BME-387).

Author contributions

Sz.P. searched for publications, digitized the data, performed the technical validation, prepared the database and wrote the manuscript. P.N.S. helped to determine the data structure of the database, revised the data description and the manuscript. B.G.M. initiated and supervised the study and wrote the manuscript.

Funding

Open access funding provided by Centre for Energy Research.

Competing interests

The authors declare no competing interests.

Additional information

Correspondence and requests for materials should be addressed to B.G.M.

Reprints and permissions information is available at www.nature.com/reprints.

Publisher's note Springer Nature remains neutral with regard to jurisdictional claims in published maps and institutional affiliations.



Open Access This article is licensed under a Creative Commons Attribution 4.0 International License, which permits use, sharing, adaptation, distribution and reproduction in any medium or format, as long as you give appropriate credit to the original author(s) and the source, provide a link to the Creative Commons license, and indicate if changes were made. The images or other third party material in this article are included in the article's Creative Commons license, unless indicated otherwise in a credit line to the material. If material is not included in the article's Creative Commons license and your intended use is not permitted by statutory regulation or exceeds the permitted use, you will need to obtain permission directly from the copyright holder. To view a copy of this license, visit <http://creativecommons.org/licenses/by/4.0/>.

© The Author(s) 2022